Magnetic Interactions at the Nanoscale in Trilayer Titanates

Yanwei Cao,[1,*] Zhenzhong Yang,[2] M. Kareev,[1] Xiaoran Liu,[1] D. Meyers,[1] S. Middey,[1] D. Choudhury,[1,3] P. Shafer,[4] Jiandong Guo,[2,5] J. W. Freeland,[6] E. Arenholz,[4] Lin Gu,[2,5] and J. Chakhalian[1]

[1]*Department of Physics, University of Arkansas, Fayetteville, Arkansas 72701, USA*
[2]*Beijing National Laboratory for Condensed Matter Physics and Institute of Physics, Chinese Academy of Sciences, Beijing 100190, People's Republic of China*
[3]*Department of Physics, Indian Institute of Technology, Kharagpur 721302, India*
[4]*Advanced Light Source, Lawrence Berkeley National Laboratory, Berkeley, California 94720, USA*
[5]*Collaborative Innovation Center of Quantum Matter, Beijing 100190, People's Republic of China*
[6]*Advanced Photon Source, Argonne National Laboratory, Argonne, Illinois 60439, USA*

(Received 1 October 2015; revised manuscript received 4 December 2015; published 17 February 2016)

We report on the phase diagram of competing magnetic interactions at the nanoscale in engineered ultrathin trilayer heterostructures of $LaTiO_3/SrTiO_3/YTiO_3$, in which the interfacial inversion symmetry is explicitly broken. Combined atomic layer resolved scanning transmission electron microscopy with electron energy loss spectroscopy and electrical transport have confirmed the formation of a spatially separated two-dimensional electron liquid and high density two-dimensional localized magnetic moments at the $LaTiO_3/SrTiO_3$ and $SrTiO_3/YTiO_3$ interfaces, respectively. Resonant soft x-ray linear dichroism spectroscopy has demonstrated the presence of orbital polarization of the conductive $LaTiO_3/SrTiO_3$ and localized $SrTiO_3/YTiO_3$ electrons. Our results provide a route with prospects for exploring new magnetic interfaces, designing a tunable two-dimensional d-electron Kondo lattice, and potential spin Hall applications.

DOI: 10.1103/PhysRevLett.116.076802

Magnetic interactions between the localized spins and conduction electrons are a fundamental component in plenty intriguing quantum many-body phenomena [1–16], a remarkable manifestation of which is the Kondo effect in heavy fermion systems [2,7–10]. Phenomenologically, in systems with localized spins coupled to conduction electrons, the Kondo interaction [1,9] competes with the magnetic Rudderman-Kittel-Katsuya-Yosida (RKKY) interaction [2] leading to the Doniach phase diagram [17,18] and Kondo lattice models [2,7,8,10]. In real transition metal compounds, however, the ground state strongly depends on the exchange interaction (J), electronic density ratio (n_m/n_c) of the localized magnetic moments (n_m) to conduction electrons (n_c), and the orbital character of magnetically active electrons [2,3,10,13,15]. In the strong-coupling regime with large $|J|$, the Kondo interaction prevails with the formation of a Kondo singlet state [1], whereas on the weak-coupling side (small $|J|$), depending on the value of n_m/n_c [3,10], the RKKY interaction may give rise to either a ferromagnetic (FM) or antiferromagnetic (AFM) order between the localized spins. In particular, in the limiting case of $n_m/n_c \gg 1$, the localized spins tend to form ferromagnetic order by polarizing the conduction electrons via the Zener kinetic exchange mechanism [3,19,20].

In correlated d-electron heterointerfaces, besides the density ratio n_m/n_c, the dimensionality and orbital polarization of the magnetic interactions are all vital components for the formation of a ground state as exemplified by the emergent FM at the manganate-cuprates [21,22] and manganite-ruthenate interfaces [23–26]. Moreover, it has been revealed that due to the significantly enhanced quantum fluctuations in reduced dimensions, under the scenario of Kondo state destruction [7,27,28] the electron and spin degrees of freedom start playing a major role to tune the heavy-fermion metal into a magnetic metal phase by crossing the quantum critical point. On the other hand, compared to f-electron heavy fermion compounds, complex oxides with partially filled d shells are believed to be the most promising candidates for high-temperature quantum materials [7], since the d-electron *orbital* configuration intimately defines their magnetic ground states [29,30]. To emphasize this, consider the splitting of the Ti t_{2g} band between d_{xy} and d_{xz}/d_{yz} subbands, which is a prime cause for the interesting emergent phenomena in the $SrTiO_3$-based heterostructures [31–38] including the coexistence of superconductivity and ferromagnetism [20,39–42], the appearance of interfacial ferromagnetism [12–15,39–46], and the formation of one-dimensional bands [14]. Since the density ratio n_m/n_c, spatial confinement, and d-electron orbital character are all important for activating novel or latent quantum states, it raises an important question: what is an experimental phase diagram for the emerging magnetic interactions at the nanoscale?

To address this challenge, we synthesized a class of asymmetric trilayer superlattices (SLs) [m u.c. $LaTiO_3/n$ u.c. $SrTiO_3/t$ u.c. $YTiO_3$] (hereafter, mLTO/nSTO/tYTO, u.c. = unit cells; see Fig. 1). In this system, the interfacial charge transfer was utilized to create a two-dimensional (2D)

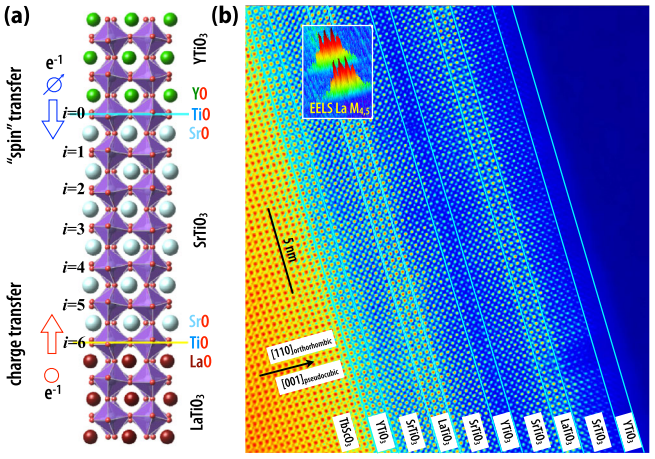

FIG. 1. (a) Schematic view of 3LTO/6STO/3YTO with two active heterointerfaces: LTO/STO and YTO/STO. Here i denotes the ith TiO_2 atomic plane of the STO layer with n unit cells. (b) HAADF-STEM image of 3LTO/6STO/3YTO. The inset is EELS spectra at the La $M_{4,5}$-edge, the three main peaks of which demonstrate the atomic sharpness of interfaces.

Fermi liquid interface (LTO/STO) and a spatially separated interface with localized magnetic moments (YTO/STO). This charge transfer across the layers was evidenced by combined scanning transmission electron microscopy (STEM) with electron energy loss spectroscopy (EELS) and electrical transport. Resonant soft x-ray linear dichroism (XLD) measurements were used to probe the orbital polarization of n_m and n_c electrons. The results have allowed us to map out the phase diagram of competing and altered magnetic interactions at the nanoscale by changing the distance between the two electronically active interfaces via the STO layer thickness n.

Trilayer SLs [3LTO/nSTO/3YTO] × 4 ($n = 2, 3, 6$) and reference samples mLTO/nSTO ($m = 3$, 20 and $n = 2$, 3, 6) and 3YTO/nSTO ($n = 2$ and 6) were epitaxially synthesized on $TbScO_3$ (110) substrates by pulsed laser deposition (PLD) with a layer-by-layer mode (see details for the growth of single layer LTO, STO, and YTO films in our previous reports) [47,48]. A JEM-ARM200F STEM, operated at 200 kV and equipped with double aberration correctors for both probe-forming and imaging lenses, was used to perform high-angle annular-dark-field (HAADF) imaging and EELS spectroscopy. The sheet resistances of the films were measured in van der Pauw geometry by the Physical Properties Measurement System (PPMS, Quantum Design). XLD at Ti $L_{2,3}$ edge with total electron yield (TEY) mode was carried out at beam line 4.0.2 (using the vector magnet) of the Advanced Light Source (ALS, Lawrence Berkeley National Laboratory).

As shown in Fig. 1(a), in the trilayer heterostructure LTO/STO/YTO there are two inequivalent interfaces composed of two rare-earth and one alkaline-earth titanate compounds (LTO, YTO, and STO) with a rich phase diagram [49]. In the bulk form, the Mott-insulator $LaTi^{3+}O_3$ (~0.2 eV gap, Ti $3d^1$) undergoes a G-type AFM phase transition below 146 K, while the Mott-insulator $YTi^{3+}O_3$ (~1.2 eV gap, Ti $3d^1$) is FM below 30 K [48,49], and, finally, $SrTi^{4+}O_3$ remains a band insulator (~3.2 eV gap, Ti $3d^0$) over the whole temperature range. The 2D conduction electrons at the LTO/STO interface [47,50], resulting from the charge transfer from the LTO into STO layers [red arrow in Fig. 1(a)], serve as the Fermi sea whereas the "spin" transfer from YTO into STO [blue arrow in Fig. 1(a)] at the other interface (YTO/STO) produces the 2D localized magnetic moments and induces spin polarization in the interface [51]. To assure that the magnetic interactions can be investigated at the unit cell scale, the interface roughness was investigated by (HAADF) STEM imaging with atomic resolution, which gives the structural projection of the SLs. Taking 3LTO/6STO/3YTO as a representative example, the geometries and sequences of the trilayer layers LTO, STO, and YTO in these SLs are clearly seen with atomically sharp interfaces as displayed in Fig. 1(b) and Fig. S1 [52].

To check for the presence of the interfacial charge transfer across the two LTO/STO and STO/YTO interfaces, the layer-resolved electronic structure of 3LTO/6STO/3YTO was investigated by atomic scale STEM-EELS line scanning across the interfaces. As seen in Fig. 2, by scanning atomic layer-resolved Ti $L_{2,3}$-edge spectra across LTO/STO and STO/YTO interfaces [along the white-dashed line in Fig. 2(a)] with high energy (0.4 eV) and spatial (0.8 Å) resolutions, the evolution of the Ti electronic structure through the interfaces was clearly observed [Fig. 2(b)]. Additionally, atomic layer-dependent line shape and peak positions of the EELS spectra carry important information regarding the interfacial charge transfer. Since each curve of the Ti $L_{2,3}$-edge spectra is a convolution of both Ti^{3+} and Ti^{4+} spectra, the spectral weight of Ti^{3+} in each spectral line of $Ti^{3+}/(Ti^{3+} + Ti^{4+})$ can track and quantify the process of interfacial charge transfer. The direct inspection of the EELS data revealed that in addition to the previously reported charge transfer from LTO into STO [31,50] there is an unexpectedly large charge transfer from YTO into STO [see Fig. 2(c)] which leads to a localized electron layer formation at the YTO/STO interface [47,51].

Next we investigated the properties of interfacial electrons (arising from the interfacial charge transfer) by measuring the temperature-dependent electrical transport. As seen in Fig. 3(a) and Fig. S2 [52], all three samples 3LTO/nSTO/3YTO ($n = 2$, 3, 6) show characteristic metallic behavior with a weak upturn at lower temperature. To investigate the conducting properties of the two interfaces (LTO/STO and STO/YTO) in the trilayer SLs and rule out possible contributions from defects and oxygen vacancies, *bilayer* YTO/STO and LTO/STO samples were synthesized and their transport properties were used as references (see Fig. S2 [52]). In sharp contrast to highly insulating YTO/STO [47,51], the sheet resistances of all

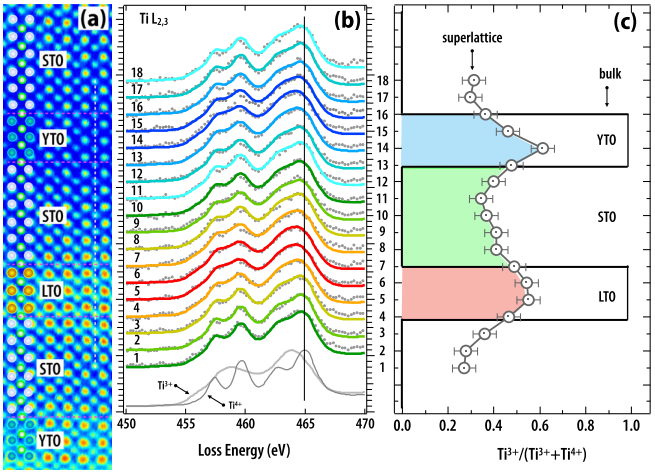

FIG. 2. (a) HAADF image of 3LTO/6STO/3YTO. The atomic positions of the elements La (large yellow dots), Sr (large white dots), Y (large blue dots), Ti (small green dots) are labeled schematically. (b) Layer-resolved EELS spectra [scanning along the dashed white lines in (a)] with the left side of the spectra aligned to the HAADF image in (a). Reference spectra for Ti^{4+} and Ti^{3+} (acquired on bulklike $SrTiO_3$ and $LaTiO_3$ films, respectively) at the bottom were adapted from Ref. [50]. The colored solid lines are the fitting curves of layer-resolved EELS spectra to a linear combination of Ti^{4+} and Ti^{3+} spectra, whereas the experimental data are marked by small gray dots. (c) Spatial decay of the Ti^{3+} signal across the two heterointerfaces. The Ti^{3+} spectra weight is estimated from the fitting parameters of solid curves in (b).

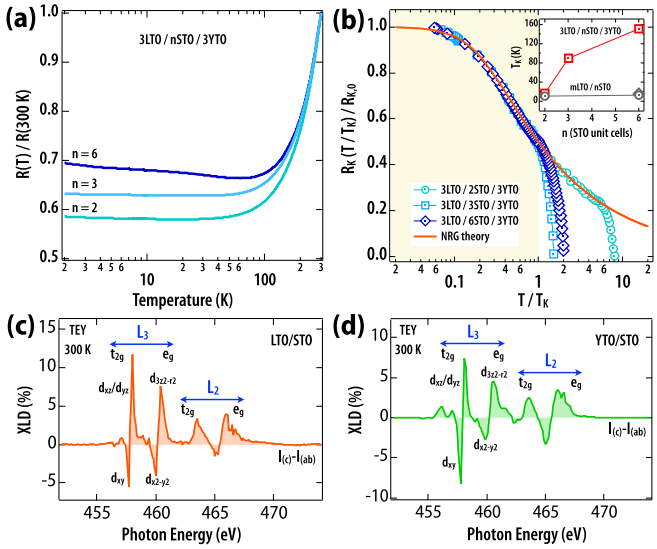

FIG. 3. (a) Normalized sheet resistances $R(T)/R(300K)$ of 3LTO/nSTO/3YTO. (b) Experimentally and theoretically [red solid line, numerical renormalization group (NRG)] scaled Kondo resistances $[R_K(T/T_K)/R_{K,0}]$ (see Eq. S4 for details). Inset, extracted n-dependent Kondo temperature T_K by fitting the experimental data of mLTO/nSTO and 3LTO/nSTO/3YTO (see Fig. S3). (c) and (d) XLD $[I(c) - I(ab)]$ of 3LTO/10STO and 3YTO/2STO interfaces with surface-sensitive TEY mode, where $I(c)$ $[E\|c$, E is the polarization vector of the photon] is for out-of-plane and $I(ab)$ $[E\|ab]$ is for in-plane detecting. It is noted most contributions of the signal are from the top few layers (STO).

the LTO/STO samples [Fig. S2(a) [52]] show a 2D electron liquid (2DEL) behavior [50,51,60–62].

With the creation of 2D conduction electrons at LTO/STO interface, the other ingredient, that needs to be considered towards the realization of controlled magnetic interactions between two separately active heterointerfaces, is the formation of localized spins at the STO/YTO junction. As highlighted by the normalized sheet resistances in Fig. S2(d) [52] (cyan shadow area, marked as T_m) and Fig. 3(a), the other dominant feature in transport is the pronounced upturn of the sheet resistances at lower temperature. Previous work on titanate heterojunctions has attributed such an upturn to the Kondo effect [12,63–66], after carefully ruling out the contributions from weak localization [67] and electron-electron interactions [68]. One of the key features of the Kondo effect that immediately differentiates it from weak-localization and electron-electron interactions is the universal scaling behavior [see Fig. S3–S4 and Eq. (S1)–(S4) [52]]. As shown in Fig. 3(b), all the *trilayer* SLs obey the Kondo scaling behavior which further affirms the dominant contribution of Kondo screening to the observed upturn feature. Based on the observation that YTO/STO interface shows massive charge transfer and yet is highly insulating, the observed Kondo behavior lends strong evidence for the formation of interfacial localized magnetic moments located on the STO side proximal to the YTO/STO interface of LTO/STO/YTO. The combined STEM/EELS and electrical transport data thus established that a 2D conduction electron layer is formed at the LTO/STO interface whereas a high-density 2D localized magnetic layer is formed in the vicinity of the STO/YTO interface (see Fig. 2 and Fig. S5 [52]).

To elucidate the link between magnetism and the d-orbital occupancy of Ti ions in the STO layer, we carried out XLD measurements to probe the orbital character of both itinerant (n_c) and localized (n_m) electrons, as shown in Figs. 3(c)–3(d) and Fig. S6 [52]. Notice, to date the study of orbital polarization and subband splitting of interfacial Ti $3d$ band by XLD were mostly carried out on $LaAlO_3/SrTiO_3$ (LAO/STO) [69–73] and very little is known experimentally about orbital physics at the LTO/STO and, in particular, the YTO/STO interface. As shown in Figs. 3(c)–3(d) and Fig. S6 [52], the orbital occupancy at both LTO/STO and YTO/STO heterointerfaces exhibits a similar configuration, where the d_{xy} subband is the lowest occupied state compared to the energy position of the d_{xz}/d_{yz} subband. This orbital configuration is in good agreement with the reported orbital physics at the LAO/STO interface [69–73].

To fully understand the magnetic interactions in LTO/STO/YTO, which strongly depend on J, n_m/n_c, and orbital polarization, the STO layer thickness (n)-dependent

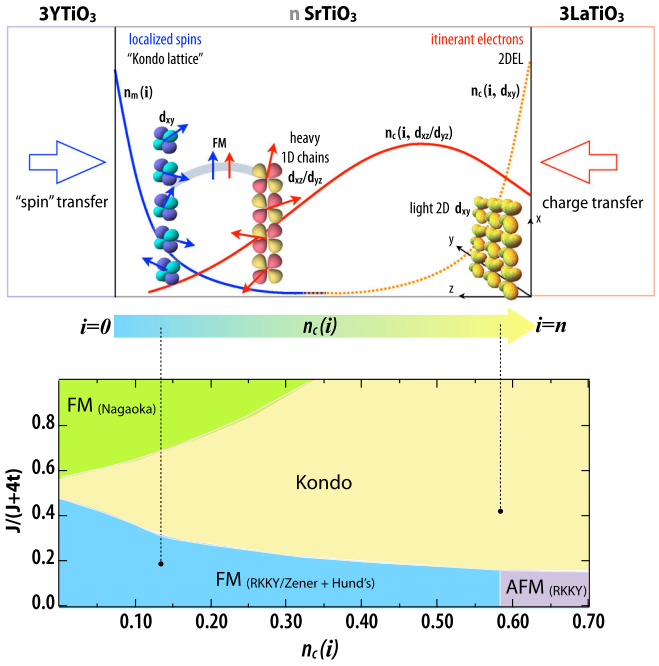

FIG. 4. Top panel, a sketch of the TiO_2 plane (i)-dependent electronic density [$n_c(i)$ for itinerant electrons and $n_m(i)$ for localized spins, $i \leq n$ [see Fig. 1(a)]] and orbital occupancy with a charge decay away from the interfaces [see also Fig. 2(c) and Fig. S5 [52]]. Bottom panel, schematic phase diagram adapted from the theory [3,10]. Near the LTO/STO interface the Kondo effect is dominant whereas ferromagnetic exchange is favored near the YTO/STO interface forming 2D d-electron Kondo latticelike structure. Note, the phase diagram is effective for both periodic and random localized magnetic moments [3,10]. Here, t is the electron hopping energy.

electronic density distribution and d-orbital occupancy were investigated. As shown in Figs. S3–S5 [52], from the combined EELS and transport data for both LTO/STO and YTO/STO interfaces, the presence of high density of 2D conduction electrons ($n_c \sim 10^{14}$–10^{15} cm^{-2}/interface) and localized moments ($n_m \sim 10^{14}$–10^{15} cm^{-2}/interface) was deduced. To demonstrate the dependence of magnetic interactions on n_m/n_c and orbital polarization we define the i-dependent carrier densities $n_c(i)$ and $n_m(i)$, where i denotes the ith TiO_2 atomic plane inside the STO layer counted from the YTO/STO interface [Fig. 1(a)]. As seen in Fig. 2(c) and Fig. S5, based on the evolution of $Ti^{3+}/(Ti^{3+} + Ti^{4+})$ ratio, both $n_c(i)$ and $n_m(i)$ show rapid decay behavior into the STO layer.

Next, we turn our attention to the orbital character of $n_c(i)$ and $n_m(i)$. Previous extensive work on STO-based heterostructures with 2DEL revealed the presence of two kinds of mobile carriers with distinct orbital dispersion, namely, light d_{xy} and heavy d_{xz}/d_{yz} electrons [13,60,74,75]. For the LTO/STO interface recent angle-resolved photoemission spectroscopy (ARPES) results [60] confirmed that light d_{xy} conduction electrons with large carrier density $n_c(i, d_{xy})$ are bound to the LTO/STO interface while away and deeper into the STO layer the mobile carriers are heavy electrons with d_{xz}/d_{yz} dispersion (see Fig. 4, top panel). On the other hand, for YTO/STO no experimental ARPES data are available. First-principles calculations predict that the YTO/STO interface is ferromagnetic and insulating [51]. A direct comparison of the XLD line shapes taken on Ti $L_{2,3}$ edge for YTO/STO, LTO/STO, and LAO/STO [69–73] lends strong support to the notion that the d_{xy} band is indeed the lowest occupied state of magnetic d electrons at the YTO/STO interface.

With the observation of $n_m(i)/n_c(i)$ and the presence of orbital polarization, it is interesting to speculate how the magnetic interactions are modulated by the STO thickness (n). We start by considering the case of a thick $n = 6$ STO layer. With a thicker STO layer, near the LTO/STO interface $n_c(d_{xy}) \gg n_m$ resulting in the formation of a Kondo singlet state, as illustrated in Fig. 4 (bottom). On the other hand, a low concentration of heavy electrons with d_{xz}/d_{yz} character disperses away from the LTO/STO interface and appears near the magnetic STO/YTO interface; upon reaching the STO/YTO interface the heavy electrons interact with the localized magnetic moments with d_{xy} character. The orbital-dependent ferromagnetic interactions then can proceed through two possible mechanisms: (i) based on Hund's rule, the interaction between the d_{xy} and d_{xz}/d_{yz} electrons results in the FM ground state [13,15] and (ii) the Zener kinetic exchange, which may win the competition with the Kondo and RKKY interactions, again leads to the formation of a localized ferromagnetic ground state with spin-polarized conduction electrons [3,10]. Based on this consideration, both Hund' s rule and Zener kinetic exchange favor the formation of localized ferromagnetism and spin-polarized conduction carriers. At the other limit, when the STO layer is ultrathin (e.g., $n = 2$), $n_c \sim n_m$ the conduction carriers lose their distinct orbital character resulting in the mixed orbital state $d_{xz}/d_{yz}/d_{xy}$. In this case the ground state is the result of a direct competition between the Kondo screening, RKKY coupling, and Hund's energy. Based on this picture, the control of STO thickness n enables the remarkable ability to modulate the critical ratio of n_m/n_c and orbital polarization to exert definitive control over the magnetic interactions.

In conclusion, we investigated the magnetic coupling between the 2D conduction electrons formed at the LTO/STO interface and the 2D localized magnetic moments at the STO/YTO interface. Because of the STO layer thickness dependent electronic density and orbital polarization of both the conduction electrons and localized spins, the competing Kondo singlet state and ferromagnetism are both present at the different TiO_2 planes inside the STO layer of LTO/STO/YTO. The strength of the magnetic interactions and the resulting magnetic ground state can be very effectively modulated by the thickness of the STO layer with nanoscale precision. Our findings provide an emerging magnetic phase diagram which should open prospects for exploring new magnetic

interfaces [13,15], designing tunable 2D Kondo lattices [7,10], and potential spin Hall applications with complex oxides [11,16,76].

The authors deeply acknowledge numerous insightful theory discussions with Andrew Millis, Se Young Park, Gregory Fiete, and Daniel Khomskii. J. C. and D. M. were supported by the Gordon and Betty Moore Foundation EPiQS Initiative through Grant No. GBMF4534. L. Gu and J. Guo acknowledge support from National Basic Research Program of China (Grants No. 2012CB921702 and No. 2014CB921002). X. L. was supported by the Department of Energy Grant No. DE-SC0012375 for his synchrotron work. Y. C., S. M., and M. K. were supported by the DOD-ARO under Grant No. 0402-17291. L. Gu and J. Guo acknowledge the support from the National Natural Science Foundation of China (51522212, 51421002, 11225422) and the Strategic Priority Research of the Chinese Academy of Sciences (Grant No. XDB07030200). The Advanced Light Source is supported by the Director, Office of Science, Office of Basic Energy Sciences, of the U.S. Department of Energy under Contract No. DE-AC02-05CH11231. This research used resources of the Advanced Photon Source, a U.S. Department of Energy (DOE) Office of Science User Facility operated for the DOE Office of Science by Argonne National Laboratory under Contract No. DE-AC02-06CH11357.

*yc003@uark.edu

[1] J. Kondo, Prog. Theor. Phys. **32**, 37 (1964).
[2] H. Tsunetsugu, M. Sigrist, and K. Ueda, Rev. Mod. Phys. **69**, 809 (1997).
[3] T. Jungwirth, J. Sinova, J. Mašek, J. Kučera, and A. H. MacDonald, Rev. Mod. Phys. **78**, 809 (2006).
[4] R. Yu, W. Zhang, H.-J. Zhang, S.-C. Zhang, X. Dai, and Z. Fang, Science **329**, 61 (2010).
[5] C. Chang *et al.*, Science **340**, 167 (2013).
[6] D. J. Kim, J. Xia, and Z. Fisk, Nat. Mater. **13**, 466 (2014).
[7] P. Coleman, Nat. Mater. **11**, 185 (2012).
[8] P. Coleman, *Handbook of Magnetism and Advanced Magnetic Materials*, edited by H. Kronmuller and S. Parkin, Vol. 1 (John Wiley & Sons, New York, 2007).
[9] A. C. Hewson, *The Kondo Problem to Heavy Fermions* (Cambridge University Press, Cambridge, England, 1993).
[10] P. Fazekas and E. Müller-Hartmann, Z. Phys. B **85**, 285 (1991).
[11] G. Y. Guo, S. Maekawa, and N. Nagaosa, Phys. Rev. Lett. **102**, 036401 (2009).
[12] A. Brinkman, M. Huijben, M. van Zalk, J. Huijben, U. Zeitler, J. C. Maan, W. G. van der Wiel, G. Rijnders, D. H. A. Blank, and H. Hilgenkamp, Nat. Mater. **6**, 493 (2007).
[13] M. Gabay and J.-M. Triscone, Nat. Phys. **9**, 610 (2013).
[14] J. M. D. Coey, Ariando, and W. E. Pickett, MRS Bull. **38**, 1040 (2013).
[15] J. Ruhman, A. Joshua, S. Ilani, and E. Altman, Phys. Rev. B **90**, 125123 (2014).
[16] C. Gorini, P. Schwab, M. Dzierzawa, and R. Raimondi, Phys. Rev. B **78**, 125327 (2008).
[17] S. Doniach, Physica (Amsterdam) **91**, 231 (1977).
[18] S. Süllow, M. C. Aronson, B. D. Rainford, and P. Haen, Phys. Rev. Lett. **82**, 2963 (1999).
[19] C. Zener, Phys. Rev. **81**, 440 (1951).
[20] K. Michaeli, A. C. Potter, and P. A. Lee, Phys. Rev. Lett. **108**, 117003 (2012).
[21] J. Chakhalian *et al.*, Nat. Phys. **2**, 244 (2006).
[22] J. Chakhalian, J. W. Freeland, H.-U. Habermeier, G. Cristiani, G. Khaliullin, M. van Veenendaal, and B. Keimer, Science **318**, 1114 (2007).
[23] J. W. Freeland *et al.*, Phys. Rev. B **81**, 094414 (2010).
[24] C. He *et al.*, Phys. Rev. Lett. **109**, 197202 (2012).
[25] A. J. Grutter, B. J. Kirby, M. T. Gray, C. L. Flint, U. S. Alaan, Y. Suzuki, and J. A. Borchers, Phys. Rev. Lett. **115**, 047601 (2015).
[26] P. Yordanov, A. V. Boris, J. W. Freeland, J. J. Kavich, J. Chakhalian, H. N. Lee, and B. Keimer, Phys. Rev. B **84**, 045108 (2011).
[27] H. Shishido, T. Shibauchi, K. Yasu, T. Kato, H. Kontani, T. Terashima, and Y. Matsuda, Science **327**, 980 (2010).
[28] Y. Mizukami *et al.*, Nat. Phys. **7**, 849 (2011).
[29] D. Khomskii, *Transition Metal Compounds* (Cambridge University Press, Cambridge, England, 2014).
[30] Y. Tokura and N. Nagaosa, Science **288**, 462 (2000).
[31] H. Y. Hwang, Y. Iwasa, M. Kawasaki, B. Keimer, N. Nagaosa, and Y. Tokura, Nat. Mater. **11**, 103 (2012).
[32] J. Mannhart and D. G. Schlom, Science **327**, 1607 (2010).
[33] F. Granozio, G. Koster, and G. Rijnders, MRS Bull. **38**, 1017 (2013).
[34] S. Stemmer and S. J. Allen, Annu. Rev. Mater. Res. **44**, 151 (2014).
[35] J. Mannhart, D. H. A. Blank, H. Y. Hwang, A. J. Millis, and J.-M. Triscone, MRS Bull. **33**, 1027 (2008).
[36] P. Zubko, S. Gariglio, M. Gabay, P. Ghosez, and J.-M. Triscone, Annu. Rev. Condens. Matter Phys. **2**, 141 (2011).
[37] J. Chakhalian, A. J. Millis, and J. Rondinelli, Nat. Mater. **11**, 92 (2012).
[38] L. Bjaalie, B. Himmetoglu, L. Weston, A. Janotti, and C. G. Van de Walle, New J. Phys. **16**, 025005 (2014).
[39] B. Kalisky, J. A. Bert, B. B. Klopfer, C. Bell, H. K. Sato, M. Hosoda, Y. Hikita, H. Y. Hwang, and K. A. Moler, Nat. Commun. **3**, 922 (2012).
[40] J. A. Bert, B. Kalisky, C. Bell, M. Kim, Y. Hikita, H. Y. Hwang, and K. A. Moler, Nat. Phys. **7**, 767 (2011).
[41] L. Li, C. Richter, J. Mannhart, and R. C. Ashoori, Nat. Phys. **7**, 762 (2011).
[42] S. Banerjee, O. Erten, and M. Randeria, Nat. Phys. **9**, 626 (2013).
[43] J. Chakhalian, J. W. Freeland, A. J. Millis, C. Panagopoulos, and J. M. Rondinelli, Rev. Mod. Phys. **86**, 1189 (2014).
[44] P. Moetakef, J. Y. Zhang, A. Kozhanov, B. Jalan, R. Seshadri, S. J. Allen, and S. Stemmer, Appl. Phys. Lett. **98**, 112110 (2011).
[45] J. Garcia-Barriocanal *et al.*, Nat. Commun. **1**, 82 (2010).
[46] S. Valencia *et al.*, Nat. Mater. **10**, 753 (2011).
[47] M. Kareev, Y. Cao, X. Liu, S. Middey, D. Meyers, and J. Chakhalian, Appl. Phys. Lett. **103**, 231605 (2013).

[48] Y. Cao, P. Shafer, X. Liu, D. Meyers, M. Kareev, S. Middey, J. W. Freeland, E. Arenholz, and J. Chakhalian, Appl. Phys. Lett. **107**, 112401 (2015).
[49] M. Mochizuki and M. Imada, New J. Phys. **6**, 154 (2004).
[50] A. Ohtomo, D. A. Muller, J. L. Grazul, and H. Y. Hwang, Nature (London) **419**, 378 (2002).
[51] H. W. Jang *et al.*, Science **331**, 886 (2011).
[52] See Supplemental Material at http://link.aps.org/supplemental/10.1103/PhysRevLett.116.076802, which includes Refs. [53–59], for details and additional data.
[53] T. A. Costi, A. C. Hewson, and V. Zlatić, J. Phys. Condens. Matter **6**, 2519 (1994).
[54] W. G. van der Wiel, S. De Franceschi, T. Fujisawa, J. M. Elzerman, S. Tarucha, and L. P. Kouwenhoven, Science **289**, 2105 (2000).
[55] J.-H. Chen, L. Li, W. G. Cullen, E. D. Williams, and M. S. Fuhrer, Nat. Phys. **7**, 535 (2011).
[56] D. Goldhaber-Gordon, J. Göres, M. A. Kastner, H. Shtrikman, D. Mahalu, and U. Meirav, Phys. Rev. Lett. **81**, 5225 (1998).
[57] M. Lee, J. R. Williams, S. Zhang, C. D. Frisbie, and D. Goldhaber-Gordon, Phys. Rev. Lett. **107**, 256601 (2011).
[58] V. Yu. Irkhin and Yu. P. Irkhin, J. Exp. Theor. Phys. **80**, 334 (1995).
[59] J. Y. Zhang, C. A. Jackson, R. Chen, S. Raghavan, P. Moetakef, L. Balents, and S. Stemmer, Phys. Rev. B **89**, 075140 (2014).
[60] Y. J. Chang, L. Moreschini, A. Bostwick, G. A. Gaines, Y. S. Kim, A. L. Walter, B. Freelon, A. Tebano, K. Horn, and E. Rotenberg, Phys. Rev. Lett. **111**, 126401 (2013).
[61] J. Biscaras, N. Bergeal, A. Kushwaha, T. Wolf, A. Rastogi, R. C. Budhani, and J. Lesueur, Nat. Commun. **1**, 89 (2010).
[62] J. Biscaras, N. Bergeal, S. Hurand, C. Feuillet-Palma, A. Rastogi, R. C. Budhani, M. Grilli, S. Caprara, and J. Lesueur, Nat. Mater. **12**, 542 (2013).
[63] G. M. De Luca *et al.*, Phys. Rev. B **89**, 224413 (2014).
[64] W.-N. Lin, J.-F. Ding, S.-X. Wu, Y.-F. Li, J. Lourembam, S. Shannigrahi, S.-J. Wang, and T. Wu, Adv. Mater. Interfaces **1**, 1300001 (2014).
[65] S. Das, A. Rastogi, L. Wu, J.-C. Zheng, Z. Hossain, Y. Zhu, and R. C. Budhani, Phys. Rev. B **90**, 081107(R) (2014).
[66] S. Das, P. C. Joshi, A. Rastogi, Z. Hossain, and R. C. Budhani, Phys. Rev. B **90**, 075133 (2014).
[67] V. F. Gantmakher, *Electrons and Disorder in Solids* (Oxford University Press, New York, 2005).
[68] S. P. Chiu and J. J. Lin, Phys. Rev. B **87**, 035122 (2013).
[69] J.-S. Lee, Y. W. Xie, H. K. Sato, C. Bell, Y. Hikita, H. Y. Hwang, and C.-C. Kao, Nat. Mater. **12**, 703 (2013).
[70] M. Salluzzo *et al.*, Phys. Rev. Lett. **102**, 166804 (2009).
[71] M. Salluzzo, S. Gariglio, X. Torrelles, Z. Ristic, R. Di Capua, J. Drnec, M. Moretti Sala, G. Ghiringhelli, R. Felici, and N. B. Brookes, Adv. Mater. **25**, 2333 (2013).
[72] M. Salluzzo *et al.*, Phys. Rev. Lett. **111**, 087204 (2013).
[73] D. Pesquera *et al.*, Phys. Rev. Lett. **113**, 156802 (2014).
[74] Z. S. Popovic and S. Satpathy, Phys. Rev. Lett. **94**, 176805 (2005).
[75] J. H. You and J. H. Lee, Phys. Rev. B **88**, 155111 (2013).
[76] T. Tanaka, H. Kontani, M. Naito, T. Naito, D. S. Hirashima, K. Yamada, and J. Inoue, Phys. Rev. B **77**, 165117 (2008).